FAME
Finnish Additive Manufacturing Ecosystem

DIMECC

FAME ECOSYSTEM White Paper

Design and Testing of Additively Manufactured 316L/Ti64/MS1 Bicycle Crank Arms

2026

Johannes Karjalainen, AMEXCI
Erin Komi, Etteplan
Markus Korpela, DIMECC

BUSINESS FINLAND

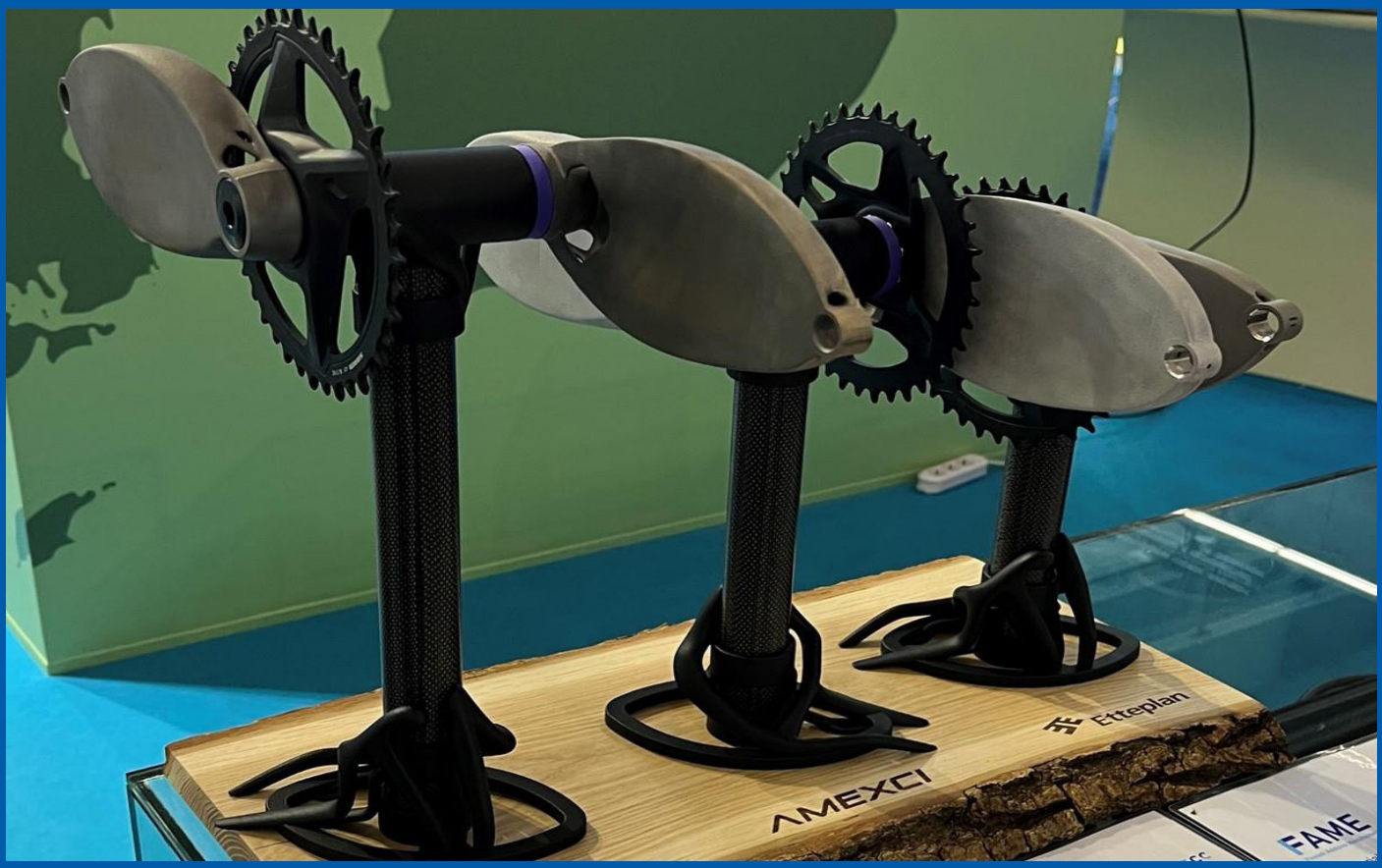

DIMECC

DIMECC PUBLICATIONS
6/2026

FAME
Finnish Additive Manufacturing Ecosystem

Images: Etteplan, AMEXCI, LUT University
Publisher - DIMECC Oy

1. Introduction

3D-printed components, like those produced by any other manufacturing methods, may end up being used in applications where they are subjected to dynamic mechanical loading. In such cases, understanding the fatigue strength properties already at the design stage is extremely important, so that the mass can be defined large enough to withstand the given load. Long-term cyclic loading can cause the component to fracture under loads several times lower than a static load of equal magnitude.

Comprehensive fatigue strength data is not widely available from additive manufacturing system manufacturers, although large multinational companies have produced such data for their own use. However, this research data is not generally accessible, and S–N curves for conventional materials cannot be directly applied, as fatigue strength is essentially process-specific due to the microstructure formed during manufacturing. Fatigue strength may also be affected by the build orientation of the components, i.e., the direction in which individual layers are produced relative to the part, heat treatments and by other post-processing methods.

In the DREAMS Co-Innovation joint project funded by Business Finland, around 10,000 3D-printed test specimens from across Finland were examined, most of which were fatigue tested. The project included testing for axial fatigue, bending fatigue, impact toughness, and tensile strength. Microstructures and powder materials were also analyzed. The project was significant even on an international scale, and the results were compiled into a national database to accelerate the development of additive manufacturing in Finland.

During the project, a separate external experiment was carried out, in which a redesigned and 3D-printed bicycle crank arm was fatigue tested based on the results obtained in the project. The arms were made from three different metallic materials: one of which had comprehensive fatigue data available from the project, while for the other two, reference values were taken from literature sources. The purpose was to validate the project results at component level.

The experiment was funded through the budget of the Finnish Additive Manufacturing Ecosystem (FAME). The design was carried out by company Etteplan, manufacturing by AMEXCI, and fatigue testing by the Steel Structures research group at LUT University. A non-scientific static test was also performed using a hydraulic press.

2. Design of the Bicycle Cranks

The design phase began by selecting materials and suitable post-heat treatments to achieve the desired material properties. The chosen materials were stainless steel EOS 316L, titanium alloy EOS Ti64, and aluminum alloy EOS Al5X1.
The loading conditions were defined using values found in various reports, articles, and standards, to ensure that the strength calculations were as realistic as possible. The fatigue load was set to 100,000 cycles, representing the number of individual load applications each crank arm would undergo. Based on this number of cycles, the fatigue strength of steel was estimated using S–N curves compiled from DREAMS project results of surface-shot-peened bending fatigue specimens, as no further surface treatments were intended to improve fatigue resistance. The fatigue strength of the titanium alloy was estimated from machine manufacturer's datasheet (as a single point rather than S-N curve) while for the aluminum alloy—being relatively new—the estimate was based on the corresponding value of a conventional reference material for the same number of cycles. In addition to the fatigue loading, static loads from two other directions were also considered.
The CAD model of the component was created using Creo CAD software. The frame and pedal connections were modeled and defined as fixed, and a volume region was created within which the final model had to fit after topology optimization. Three loading directions were defined, which, together with the volume region and fixing points, are shown below (Figure 1).

The first load case and direction (LC1) was defined as a horizontal peak load applied through the pedal, representing the worst possible scenario. The second load case (LC2) was defined as a constant cyclic load applied at a 45-degree angle.
At this stage, it was already possible to estimate the manufacturing orientation of the component quite accurately, i.e., the part's orientation relative to the build platform during printing. The greater mass concentration would be on the side with the larger mounting hole (the crank axle attachment), making a vertical build orientation the most logical choice to minimize support structures. The number of supports was expected to be minimal, since no overhanging structures were anticipated that could not be eliminated by slight geometric adjustments. Some supports were assumed to be necessary in the axle mounting hole, as the overhanging region at the top of the hole would otherwise be too large.
The first geometry versions of the component were created using topology optimization. The goal of the topology optimization was to maximize the stiffness of the part while achieving a mass between 5% and 30% of the defined volume region. The software was also given the loading conditions and a safety factor.

2. Design of the Bicycle Cranks

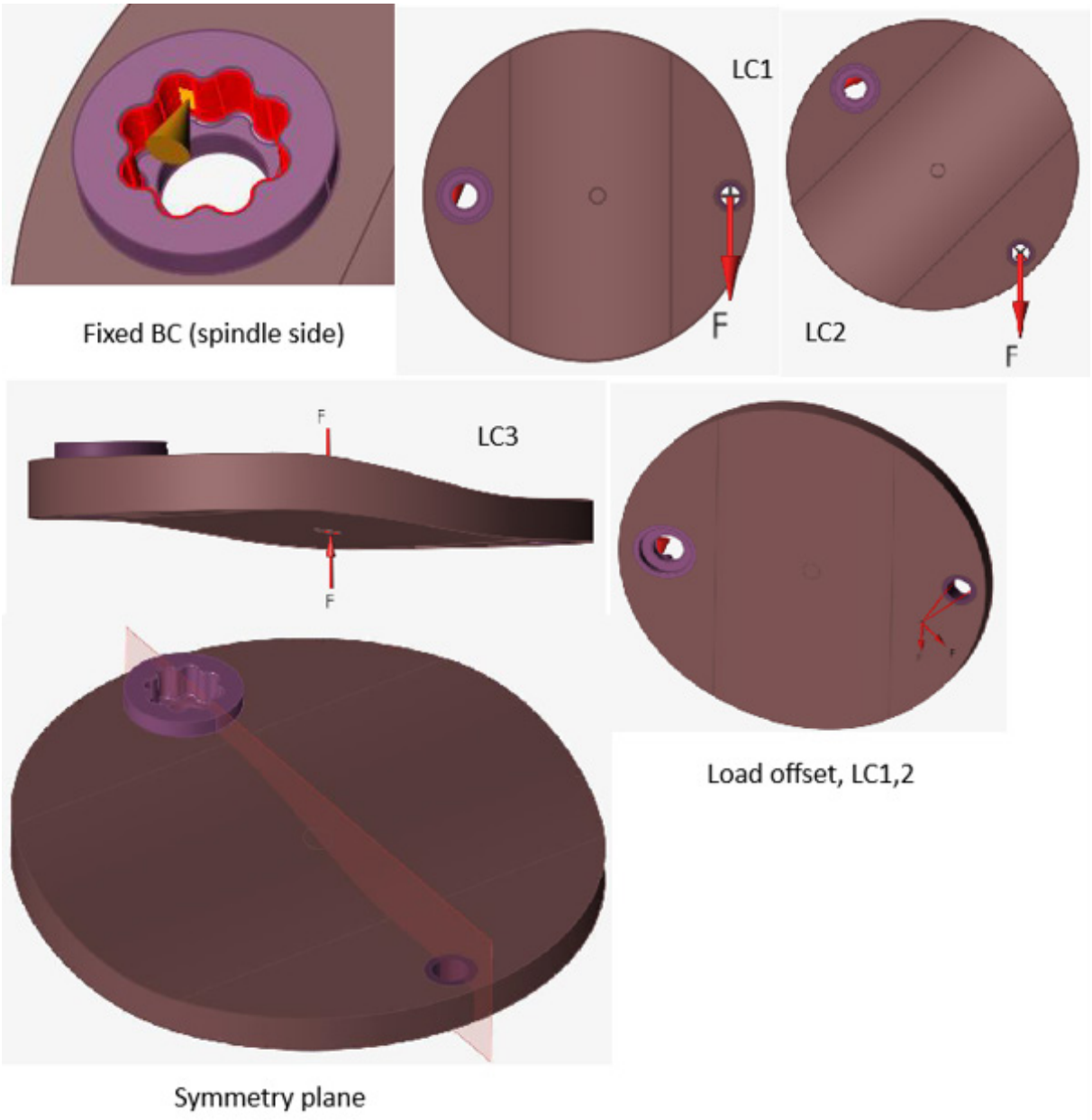

Figure 1. Load areas and directions, pedal attachment points, and volume region.

2. Design of the Bicycle Cranks

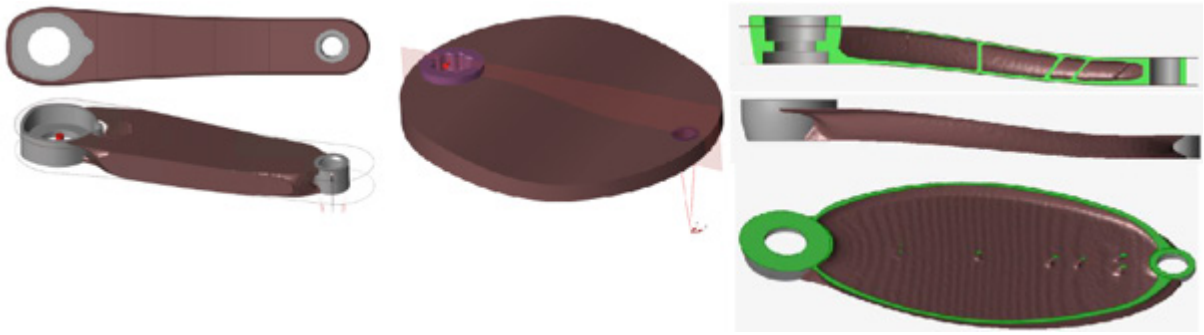

Figure 2. Different geometry alternatives generated by the software on both sides of the central volume model.

From a manufacturing standpoint, constraints were set for the minimum feature thickness and the maximum allowable unsupported overhang angle. For the strength calculations, the material properties defined for the software included Young's modulus, Poisson's ratio, density, yield strength, and fatigue strength.

As material property values for the heat-treated components, the manufacturer's stated values were used, excluding fatigue strength data. The values of the manufacturing constraints were varied, and different volume model alternatives were tested in the software to achieve varying geometries. Collaboration with the manufacturing partner was particularly important at this stage of the design process to ensure that accurate values for the manufacturing constraints could be applied. The software generates the geometry based on strength calculations, which also automatically provides a FEM analysis of the component. For each material, several geometry alternatives were created, from which the final options shown below (Figure 3) were selected. The goal was to select a geometry suitable for all three materials, requiring only minor material-specific adjustments. The selection process utilized Altair's tools Inspire PolyMesh and Inspire PolyNURBS.

The results of the chosen topology optimization were imported into the former as an STL file, including the defined attachment points. Next, a so-called voxel mesh was created with the software, enabling modifications to be merged into the model, after which it was

2. Design of the Bicycle Cranks

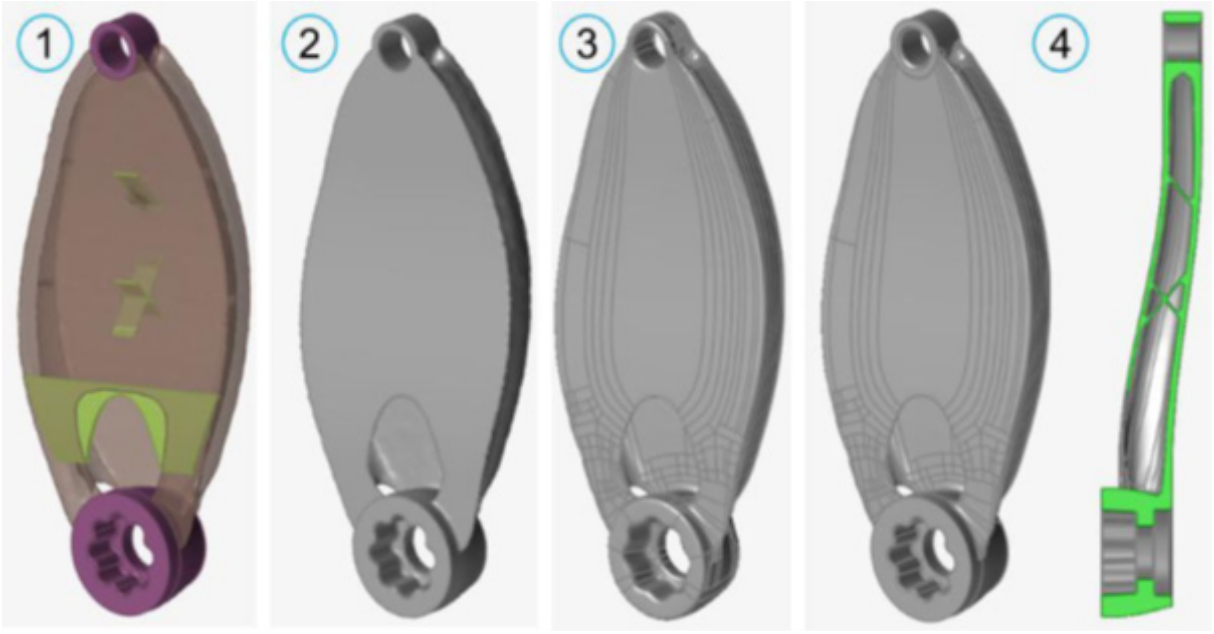

Figure 3. Selected geometry alternatives from the options generated by the software. 1) Optimized results plus features to help with printability 2) Shrinkwrap mesh (PolyMesh) 3) PolyNURB with symmetry 4) Component finalized in Creo.

exported as a unified STEP model.
A unique optimized design for each material was used as the required volume of material changed depending on the material strength. The models were finalized using Creo. The pedal mounting hole was removed, as it would be more practical to drill it during post-machining. The locations of the support structures were verified using Materialise Magics software. Supports were expected to be required between sections of the part and inside the axle mounting point to support the hole.
In the final strength analysis, the stresses were compared once more with the estimated fatigue strength values and assessed from a practical standpoint—whether the stresses were compressive or tensile, which areas they affected, and whether they might cause issues in subsequent post-processing. Potential problems could include, for instance, stresses located in regions inaccessible to shot peening, such as internal structures. Another concern could be high tensile stress peaks in areas where fatigue cracking would otherwise be most likely to occur.
Manufacturing feasibility was simulated. The

2. Design of the Bicycle Cranks

material properties defined for the simulation were the same as those used in topology optimization, except that as-built property values and layer thickness information were applied instead of the heat-treated ones.
The simulation results showed that the crank arm would experience slight distortion due to heat input during manufacturing, though not to an extent that would risk premature build failure. The support structures could not be too delicate; they needed to be sufficiently robust to conduct heat and to keep the part fixed in place despite the distortion. The parts were planned to be cut off the build platform using a bandsaw, requiring support structures at least a few millimeters thick between the part and the platform to prevent the saw from damaging the part itself.
Based on the results, the manufacturing partner was instructed to create robust support structures using their empirical experience.
The manufacturer also 3D-printed calibration specimens, which were used to create the material profile in the Amphyon simulation software so inherent strain method could be utilized.
All models were hollow structures and externally very similar. Their masses and volumes

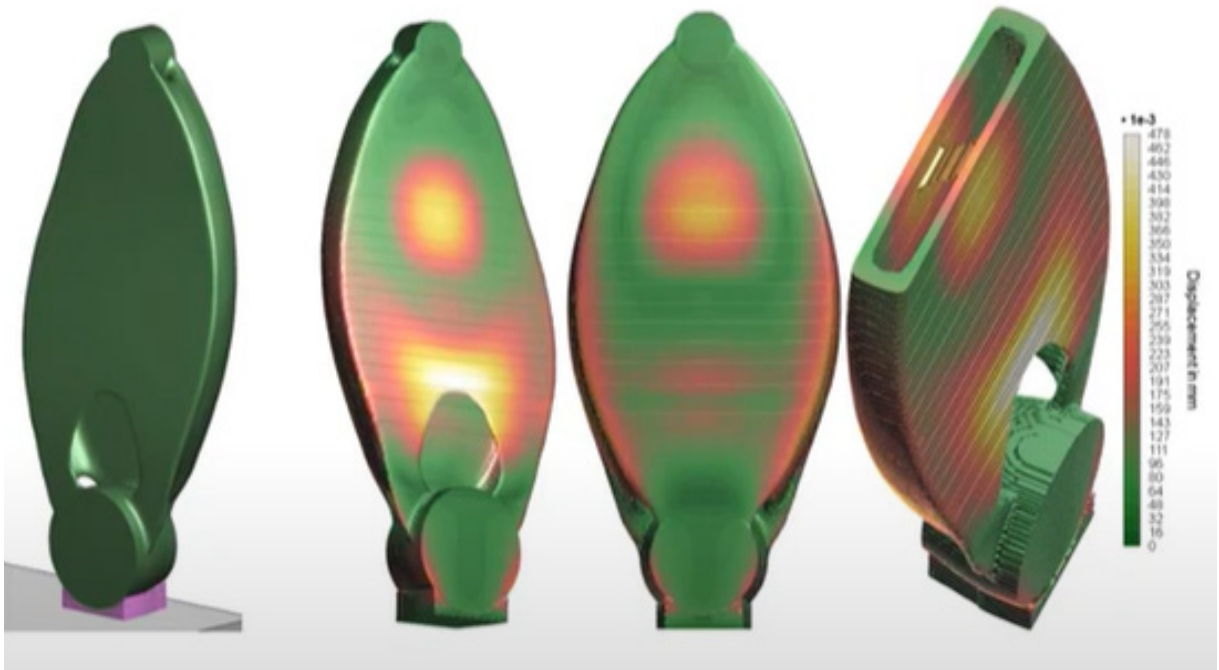

Figure 4. Results of the manufacturing simulation.

2. Design of the Bicycle Cranks

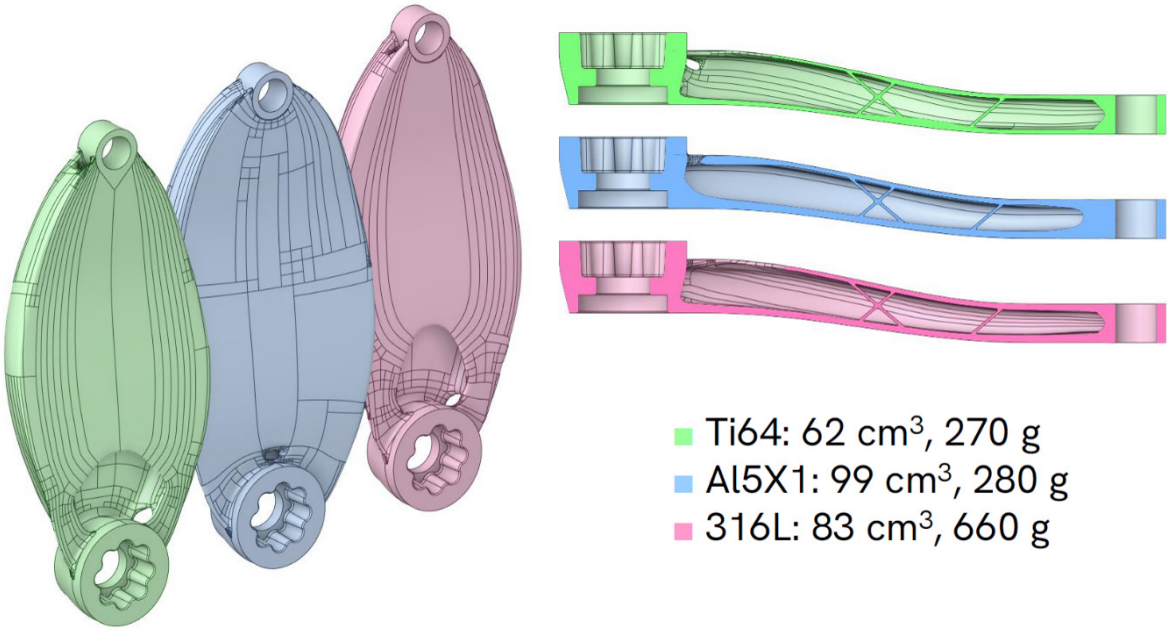

Figure 5. Final 3D models for different materials.

are presented below (Figure 5).
A unified set of technical documentation was created for the models using two technical drawings. The drawing shown below (Figure 6) was intended for 3D printing, while the following one (Figure 7) was prepared for post-processing.

2. Design of the Bicycle Cranks

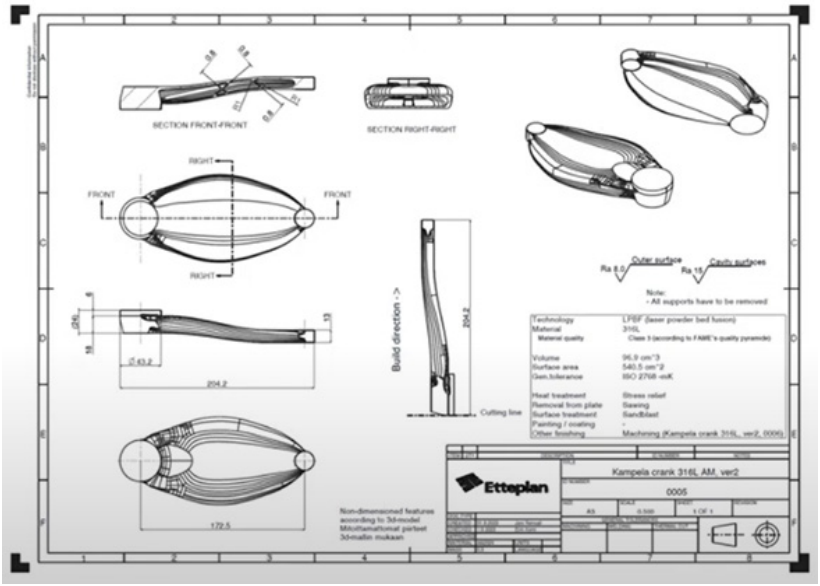

Figure 6. 3D printing drawing for the created models.

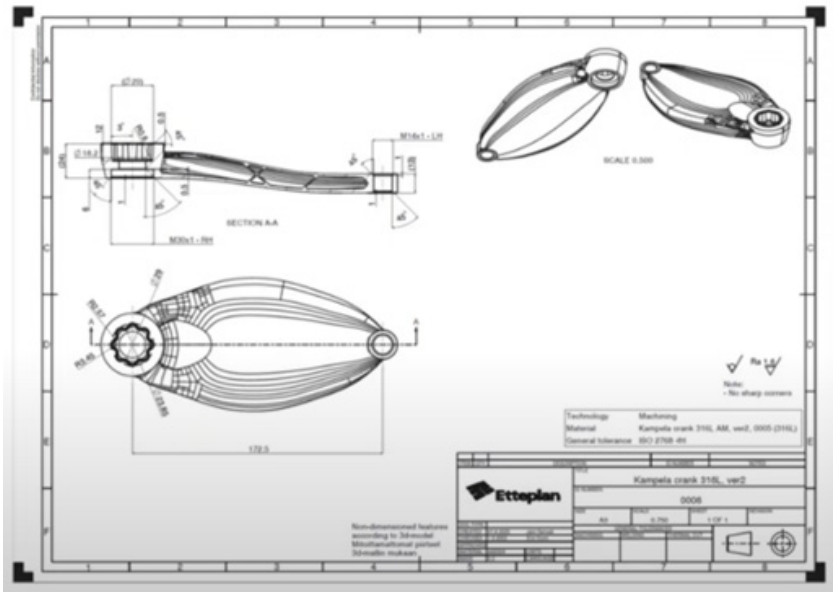

Figure 7. Post-processing drawing for the models.

3. Manufacturing

The components were manufactured at AMEXCI's facilities in Lempäälä based on the technical documentation provided by Etteplan. For the manufacturing process, AMEXCI created reinforced support structures for the parts using Materialise Magics software, following the given guidelines.
The material mixing history was known, and for these builds as well, information about the materials used was documented for potential further review.
After the builds were completed, manufacturing reports were obtained from the machine, confirming that the process conditions had been as intended. A manual powder removal process was carried out inside the build chamber, during which most of the unused powder material was removed from around the parts to allow them to be lifted out together with the build plate while minimizing powder dispersion into the surrounding environment.
The parts were then transferred to a separate blasting cabinet, where more detailed manual powder removal was performed using a pneumatic tool.
In the next step, the parts and the build plate were placed in a furnace for heat treatment to relieve residual stresses from manufacturing

Figure 8. Image of a single build with the parts.

Figure 9. Identification number of the powder batch visible on the lid of the material container. (Image: AMEXCI Oy)

3. Manufacturing

and to achieve the desired mechanical properties. During this process, any partially melted or adhered powder particles on the part surfaces were also sintered. The furnace temperature was monitored not only by the machine's internal sensor but also by an additional calibrated sensor to ensure the accuracy of the heat treatment. Temperature reports from the furnace were verified against readings from a second thermometer.

After heat treatment, the parts were cut off the build plate using a bandsaw. The remnants of the support structures between the parts and the build plate, as well as those around the axle mounting area, were then manually removed and ground smooth.

As the powder material is hazardous to health, the final processing step involved cleaning the parts in an ultrasonic bath to remove any remaining residues, after which the parts could be handled safely without protective equipment.

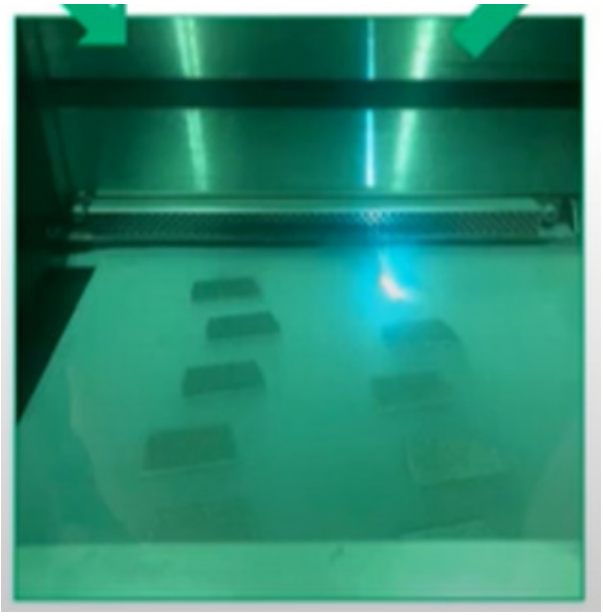

Figure 10. Completion of the parts inside the build chamber. (Image: AMEXCI Oy)

4. Testing

The parts were tested both scientifically and non-scientifically. The scientific tests were fatigue tests carried out by the Steel Structures Research Group at LUT University and the results published in scientific article called Effect of design optimization and material selection on the fatigue performance and fracture mechanism of a crank arm https://doi.org/10.1016/j.prostr.2025.06.152.
The non-scientific static tests were performed in a now-defunct machine shop using a hydraulic press operated by Lauri Vuohensilta, known from the YouTube channel Hydraulic Press Channel. An entertaining video of this test was published on YouTube (Hydraulic Press Channel).
The static test was conducted by applying force from a hydraulic press to an axle bolted to the pedal mounting point. In the fatigue testing, the dynamic load was also applied through an axle bolted to the pedal mounting point.

Figure 11. An entertaining video of the non-scientific test was published on YouTube (Hydraulic Press Channel).

5. Results

In the non-scientific static test, the crank made from steel began to deform under a load of 1,400 kg (13.7 kN) but did not fracture, which is typical for materials with high elongation at break. The crank made from titanium alloy fractured at a load of 1,100 kg (10.8 kN), and the one made from aluminum alloy fractured at 700 kg (6.87 kN).

Using these results, Etteplan conducted an additional FEM analysis in three different ways, and the results are presented below (Figure 12).

The FEM analysis results consistently reflected the findings of the static test. In the image showing compressive and tensile stresses, the orange areas represent tensile stresses and the green areas represent compressive stresses. In the Major Principal Stress and Von Mises plots, the red regions indicate stress values exceeding the material's ultimate tensile strength. In the test, the component fractured exactly at the location where the analysis predicted the highest tensile stress concentration (circled in red).

The exact fracture locations differed slightly from the simulated ones for the titanium and aluminum components, but they were still within the predicted regions. The steel

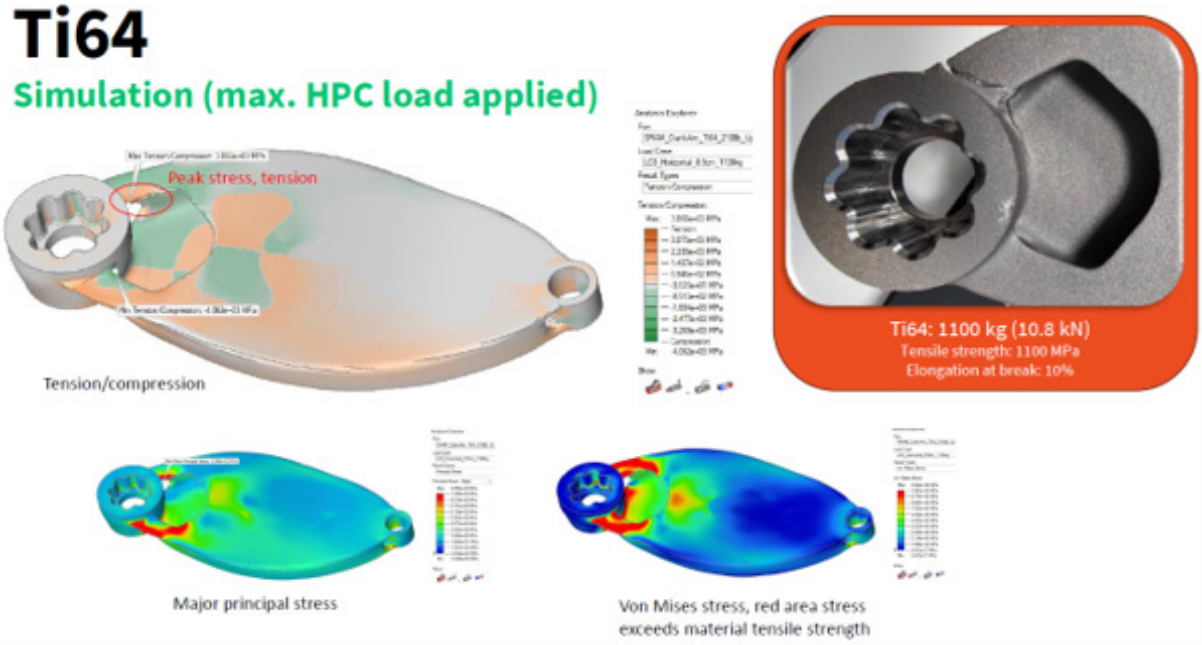

Figure 12. FEM analysis results of the titanium alloy component under static loading using three different methods. (Image: AMEXCI Oy & Etteplan Oyj)

5. Results

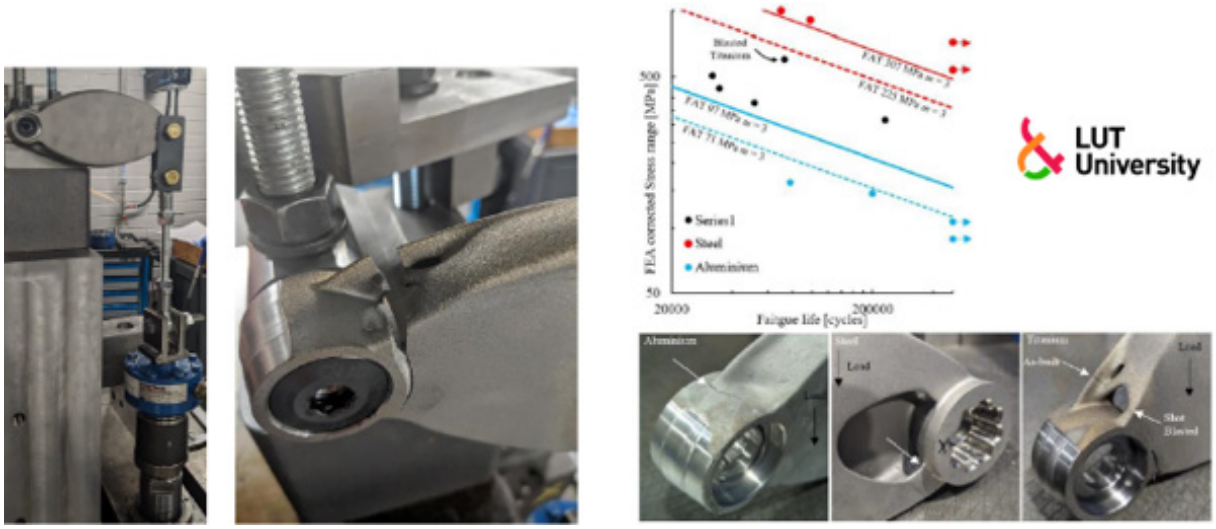

Figure 13. Fatigue test at LUT University.

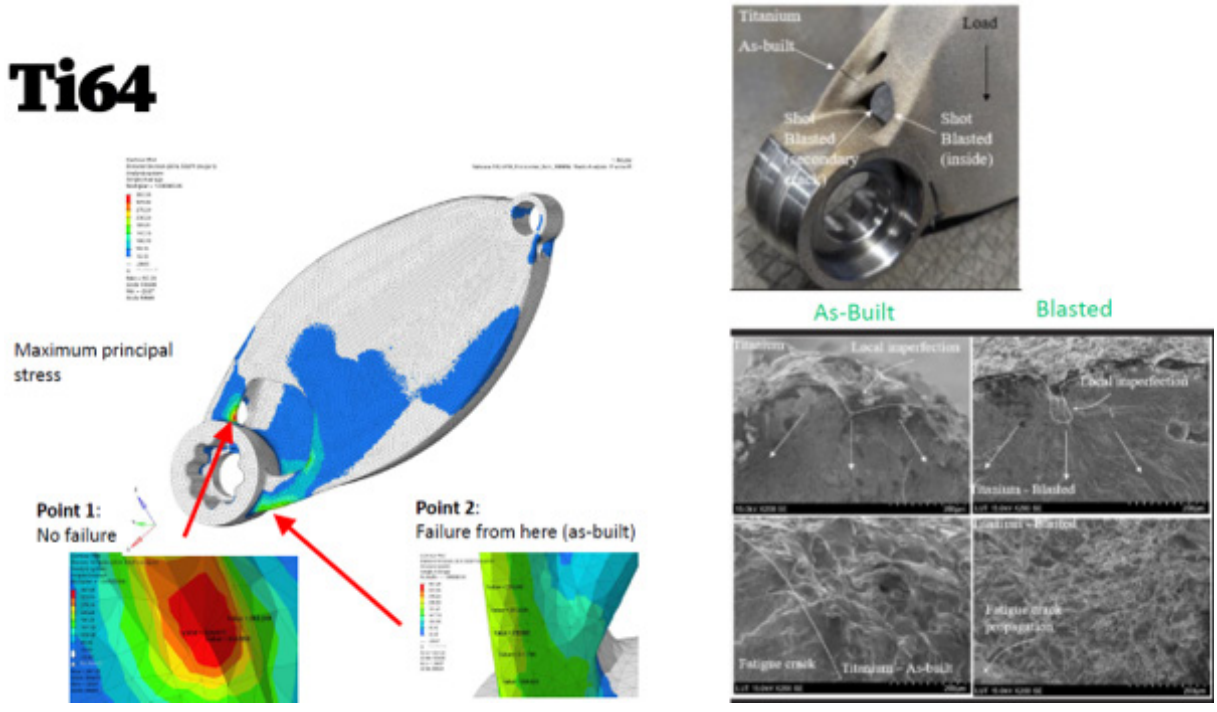

Figure 14. Titanium part

5. Results

component failed as expected. The fatigue strengths of the titanium and aluminum parts had been overestimated due to the lack of relevant S–N curves, which caused the fatigue fractures to occur at lower cycle counts than expected. For the steel component, the measured fatigue strength corresponded precisely with the design values.

The first fatigue-tested titanium component fractured in the expected region, but not at the exact predicted spot. Researchers at LUT University observed from electron microscope images that the fracture had initiated at a surface area whose texture did not match what it should have been after shot peening. Shot peening induces compressive residual stresses on the surface of the component, which increases fatigue strength. Before fatigue testing the second component, the shot peening was performed more carefully in the same region, resulting in the fracture occurring elsewhere. However, even this time the fracture did not appear at the simulated location, but rather in a similar area as in the first test piece — one that the shot peening had not effectively reached.

Such local defects cannot be accounted for in FEM analysis, which assumes a fully homogeneous structure throughout the part. It is also possible that excessive heat input contributed to the fracture locations — a common issue for geometries where a thin structure supports a region with higher mass. However, this problem is gradually being eliminated as equipment adaptivity becomes more common. Adaptivity allows the laser power directed

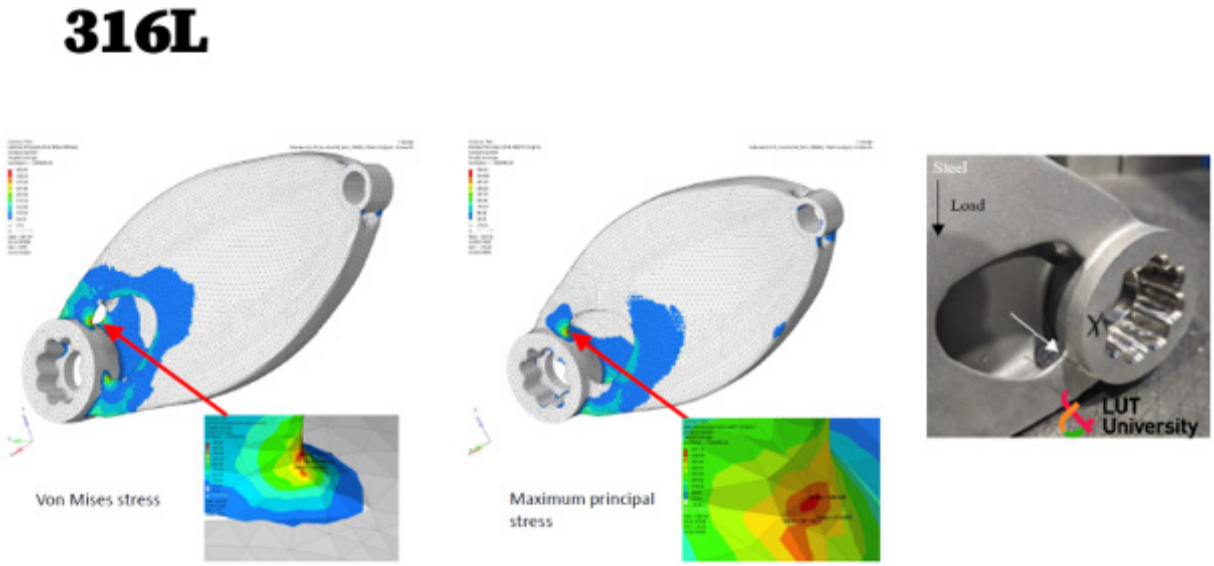

Figure 15. Stainless steel part.

5. Results

to the melt pool to be automatically reduced whenever the risk of overheating is detected in real time.

The fracture location was also affected by an overly optimistic fatigue strength value used in the design phase, which led to an insufficient wall thickness. If this had been an actual production component, the thin section could have easily been avoided by slightly increasing material thickness in that area. The resulting cost increase would have been negligible in the overall context but would have eliminated a complete risk factor.

Overall, the experiment can be considered successful, as only one iteration was needed, and the S–N curves created during the DREAMS project using test specimens were proven to be relevant for acid-resistant stainless steel.